

# Electrical Properties of Poly(Butylene Terephthalate)

FRANCO SANDROLINI, ANTONIO MOTORI, and ANDREA SACCANI

Dipartimento di Chimica applicata e Scienza dei materiali-Facoltà di Ingegneria, Università di Bologna, Bologna, Italy

## SYNOPSIS

Direct current (dc) and alternating current (ac) electrical properties of semicrystalline poly(butylene terephthalate) (PBT) are investigated as a function of temperature and frequency.

Dc electrical conductivity measurements have been performed over the temperature range  $-75^{\circ}\text{C}$  to  $130^{\circ}\text{C}$  and point out an essentially ionic mechanism of charge transport. Charge carriers are identified in protons supplied by ionization of carboxyl end-groups after dissociation of the existing hydrogen bonds.

Dielectric constant and loss factor have been measured over the temperature range  $-100^{\circ}\text{C}$  to  $130^{\circ}\text{C}$  and over the frequency range  $10^{-6}$  to  $10^6$  Hz. Together with dc measurements, they allow the detection of the  $\alpha$  glass-rubber and the  $\beta$  subglass relaxation processes, as well as an interfacial polarization of the Maxwell-Wagner-Sillars type.

Finally, the contour map of loss factor, summarizing the overall dielectric behavior of the polymer, is reported and discussed for electrical applications of PBT.

## INTRODUCTION

Engineering thermoplastic polyesters are widely used due to combination of excellent physical, thermal, mechanical, and electrical properties combined with satisfactory processing characteristics (fast processing cycles and excellent mold flow). Among these polyesters, poly(butylene terephthalate) (PBT) is mainly used in automotive, electrical, electronic, and other engineering applications and is acquiring more and more importance due to its processing advantages in comparison with poly(ethylene terephthalate) (PET). In fact, it crystallizes more rapidly than PET and does not need nucleating agents, thus allowing short extrusion and injection-molding cycles and dimensionally stable products to be obtained. Several results on the electrical behavior of PBT were reported in previous papers,<sup>1-5</sup> such as dc electrical conductivity, dielectric constant, and dielectric loss factor (and hence dielectric relaxation processes) of as-synthesized PBT as a function of temperature, frequency and crystallinity.<sup>1-3</sup> Dc investigations pointed out an essentially ionic conduction mechanism for semicrys-

talline PBT, while ac investigations pointed out several molecular relaxation processes.<sup>4</sup> Finally, dynamic-mechanical investigations allowed the resolution of finer relaxation processes, depending on the unidirectional and bidirectional stretching of material.<sup>5</sup>

The purpose of this paper is to investigate the electrical properties of PBT over a wide range of temperature and for ac properties, over a wide frequency range, in order to obtain a deeper knowledge of the behavior for engineering applications by means of an exhaustive map of dielectric relaxation processes.

## EXPERIMENTAL

### Material and Samples

PBT free from additives and stabilizers (supplied by Montedison) had the following characteristics:<sup>2,3</sup> glass transition temperature  $T_g = 22^{\circ}\text{C}$ ; melting point  $T_m = 220^{\circ}\text{C}$ ; intrinsic viscosity at  $30^{\circ}\text{C}$  in a phenol-tetrachloroethane mixture  $[\eta] = 1.00$  dL/g; number-average molecular weight  $M_n = 26,000$ ; carboxyl terminals  $80 \text{ g}_{\text{eq}}/10^6 \text{ g}$ ; ash 200 ppm.

Specimens were molded under vacuum at  $260^{\circ}\text{C}$  in the form of disks 0.3 to 3.0 mm thick and 25 mm

in diameter. At this temperature, significant thermal degradation phenomena do not occur, and memory effects of the previous structure are not present.<sup>3</sup> Before electrical measurements, specimens were vacuum annealed at 205°C for 16 h. After this treatment the polymer exhibited a crystallinity of about 60%, as determined by density measurements with a titration method in a toluene/carbon tetrachloride solution.<sup>6</sup> Other samples were quenched from the molten state in an ice-water mixture in order to obtain highly amorphous specimens.<sup>3</sup> Mixtures exhibiting lower temperature were not so effective as the ice-water mixture for quenching, due to the formation of a thermally insulating vapor layer on the sample surface.

Due to fast crystallization of PBT, amorphous and semicrystalline samples were stored at -20°C and room temperature, respectively, in a dry and dark environment under vacuum until measurements, in order to avoid crystallinity changes.

### Electrical Measurements

Dc charging currents were measured as a function of time by the voltmeter-ammeter method according to ASTM Standard D 257 with the three-terminal cells and instrumentation elsewhere described<sup>2,7</sup> by applying a constant electrical field ranging from 0.6 to 91 kV cm<sup>-1</sup> in the temperature range -75°C to 130°C. Hence, current-voltage characteristics, as well as dc electrical conductivity  $\gamma$  as a function of reciprocal absolute temperature, were obtained. Moreover, dc discharging currents were measured as a function of time to detect possible dielectric relaxation effects in the ultra-low frequency range (< 10<sup>-2</sup> Hz) by the Hamon data treatment method and its improvements.<sup>8-12</sup> Discharging currents measurements were started when quasi-steady-state values of the charging currents were obtained, in order to avoid systematic errors in the analysis of discharging transients.<sup>13,14</sup>

Ac measurements were performed according to ASTM Standard D 150 with the three-terminal cells and instrumentation elsewhere described.<sup>2,7,15</sup> Measurements were made over the frequency range 10<sup>-2</sup> to 10<sup>5</sup> Hz and temperature range -100°C to 130°C. Relative dielectric constant and loss factor as a function of frequency and temperature were thus obtained.

Before measurements, specimens were gold coated by vacuum deposition, in order to obtain the suitable three-terminal electrode configuration. All measurements were made in a dynamic vacuum from the highest to the lowest temperature, to minimize

the effects of accidental adsorption of gases or vapors on the sample surfaces.

In order to investigate the effect of moisture on the electrical properties of PBT, some samples were conditioned in water saturated air at room temperature for a variable time: samples with absorbed water contents up to 0.46 wt % were so obtained, and were subjected to dc and ac measurements in a closed environment at 25°C.

## RESULTS AND DISCUSSION

The dc electrical conductivity  $\gamma$  at 1, 10, and 60 min after the application of a step voltage is plotted in Figure 1 as a function of reciprocal absolute temperature in the temperature range -75 to 130°C and under an applied electrical field of 45.5 kV cm<sup>-1</sup>. As can be seen, the electrical conductivity exhibits a nonlinear behavior and transient phenomena, increasing with decreasing temperature, occur at all the investigated temperatures. The conductivity values vary approximately between 10<sup>-14</sup> S/cm at 130°C and 10<sup>-18</sup> S/cm at room temperature and are typical of excellent insulating materials. Measurements performed in air at 25°C on specimens with variable contents of absorbed water revealed that conductivity increased with water content: conductivity (at 1 min after voltage application) increased about four times for a water absorption of 0.46 wt %, as shown in Table I.

The behavior and values of electrical conductivity are substantially independent of the electrical field in the investigated range, i.e. 0.6 to 91 kV cm<sup>-1</sup>, up to 105°C, while the values change above this tem-

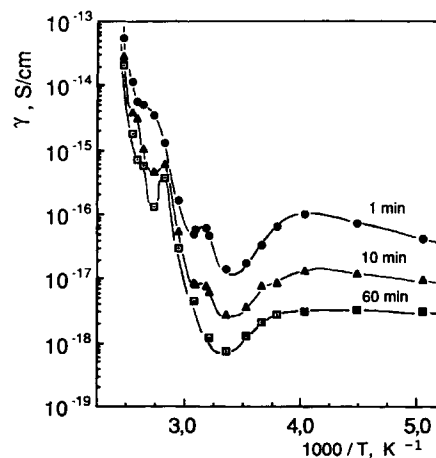


**Figure 1** Electrical conductivity  $\gamma$  as a function of reciprocal absolute temperature.

perature due to the deviation of current-voltage characteristics from linearity. Current-voltage characteristics (not shown for the sake of brevity) exhibit indeed a true ohmic trend up to 105°C, while at higher temperatures average slope decrease and deviations from linear behavior increasing with temperature occur.

The relatively weak fields and the analysis of the charging and discharging currents transients made it possible to rule out space charge effects arising from injection and trapping of charge carriers.<sup>2</sup> Moreover, measurements made with different electrode metals (Au, Al) allowed to exclude electrode blocking effects.<sup>2</sup>

The isochronal discharging currents of semicrystalline PBT are plotted in Figure 2 as a function of temperature. Remarkable transient phenomena are exhibited at all temperatures.

Furthermore, three peaks are present in the discharging curves: two of them are found at about -25°C and 40°C, respectively, and their position is practically independent of discharging time, while the third peak ranges from 70 to 105°C as a function of the discharging time. The same processes can be observed also in the conductivity curves of Figure 1, as well as in the corresponding charging currents, but are less detectable due to the superposition of the conduction currents, which may mask these effects.

The ultra-low ( $< 10^{-2}$  Hz) frequency data obtained by the Hamon treatment of the dc discharging currents of Figure 2 are reported in Figure 3. A relaxation process, whose maximum shifts to higher frequencies as temperature increases, can be observed. This process has been related to the temperature-dependent peak of Figures 1 and 2 and can be ascribed to an interfacial polarization of the Maxwell-Wagner-Sillars (MWS) type.<sup>2</sup>

The same measurements were also performed on highly amorphous PBT from room temperature to 66°C (higher temperatures would induce prompt crystallization), in order to analyze the effect of

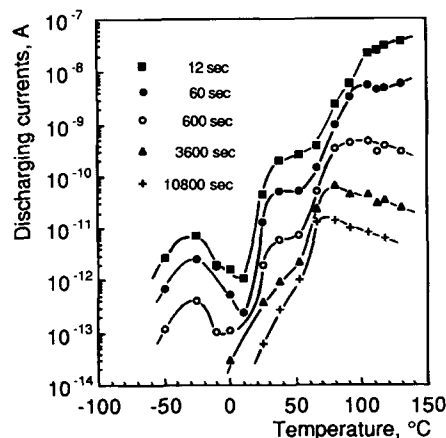


Figure 2 Discharging currents vs. temperature.

morphology on the dc behavior of the polymer. The results in terms of dc electrical conductivity are shown in Figure 4: higher conductivity was detected for the amorphous samples in comparison with the semicrystalline ones under the same conditions of time and temperature; moreover, steady-state values were observed in the amorphous samples at the highest temperature. As previously reported, the Hamon treatment of the dc discharging currents showed the same relaxation process observed in Figure 3 for the semicrystalline samples with an intensity of about one order of magnitude lower.<sup>3</sup>

The results of ac measurements are reported in Figures 5 and 6, where dielectric constant and loss factor, respectively, are plotted as a function of temperature and frequency. Dielectric constant (Fig. 5) increases with increasing temperature and decreasing frequency from 2.85 at  $3.3 \times 10^5$  Hz and -100°C to 3.95 at  $2 \times 10^{-2}$  Hz and 105°C. Loss factor curves (Fig. 6) exhibit two relaxation peaks which shift to

Table I Electrical Conductivity as a Function of Absorbed Water Content

Wt %	$\gamma$ , S/cm	
	1 min	10 min
0 (Vacuum)	$1.12 \times 10^{-17}$	$2.11 \times 10^{-18}$
0.13	$1.23 \times 10^{-17}$	$2.18 \times 10^{-18}$
0.46	$4.35 \times 10^{-17}$	$6.81 \times 10^{-18}$

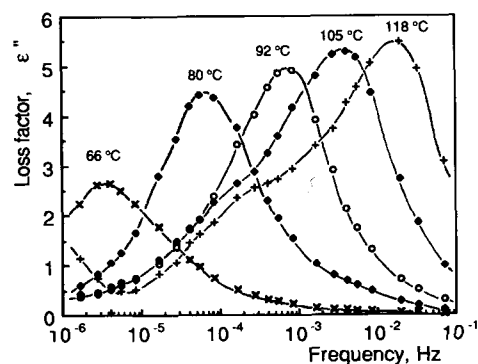
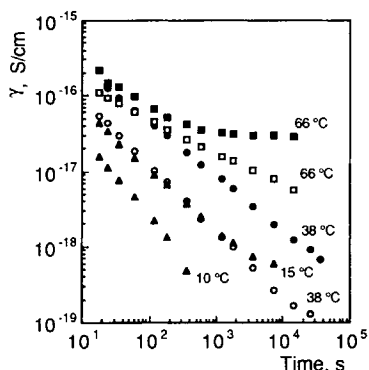


Figure 3 Loss factor vs. frequency.



**Figure 4** Electrical conductivity of semicrystalline (empty symbols) and amorphous (black symbols) PBT vs. time.

higher temperatures at increasing frequencies. The low-temperature peak corresponds to the so-called  $\beta$  (local) relaxation process, while the high-temperature one, much narrower and higher in magnitude, is relevant to the  $\alpha$  glass-rubber transition relaxation of the amorphous phase.<sup>3-5</sup> Measurements performed on quenched PBT showed that both these processes are enhanced by the increase of the amorphous content.<sup>3</sup> The  $\beta$  and  $\alpha$  relaxations processes are clearly related to the peaks observed in Figures 1 and 2 at about  $-25^\circ\text{C}$  and  $40^\circ\text{C}$ , respectively. Furthermore, rise of dielectric constant and loss factor can be observed in the high-temperature region for low frequency values, which can be ascribed to the already cited interfacial polarization of the Maxwell-Wagner-Sillars type.

The so-called transition map for the relaxation processes of Figures 3 and 6, obtained by plotting the frequencies of the maxima  $f_m$  (from isothermal loss factor curves) as a function of reciprocal absolute temperature, is reported in Figure 7. As can

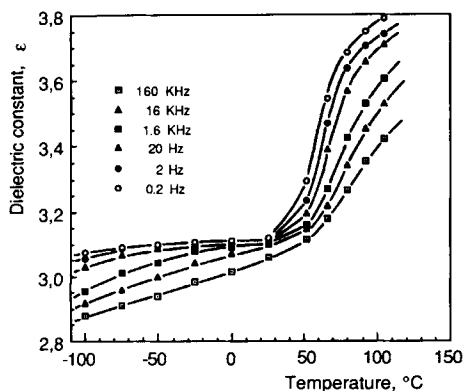


**Figure 5** Dielectric constant vs. temperature at different frequencies.

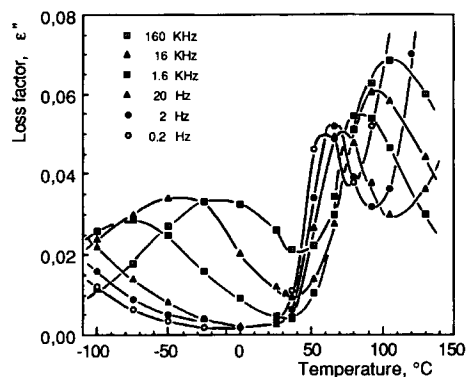


**Figure 6** Loss factor vs. temperature at different frequencies.

be seen, these processes are thermally activated with very different apparent activation energy: values of  $483 \text{ kJ mol}^{-1}$ ,  $27 \text{ kJ mol}^{-1}$ , and  $232 \text{ kJ mol}^{-1}$  can be derived for the  $\alpha$ ,  $\beta$  and ultra-low frequency polarization respectively. The values for  $\alpha$  and  $\beta$  relaxation are, indeed, somewhat different from those elsewhere reported:<sup>16,17</sup> this could be due to the different material characteristics (crystallinity, presence of additives (mainly plasticizers), etc.), and electrical measurement atmosphere. Deviation from linearity can be observed for the  $\beta$  process at the highest temperatures, which can be related to deviation from ohmic behavior observed in dc measurements. In Figure 7 the transition map for the  $\beta$  relaxation of the highly amorphous polymer is also reported. A temperature dependence very close to that of the corresponding process in the semicrystalline PBT and about the same activation energy,  $34 \text{ kJ mol}^{-1}$ , can be observed.

Dielectric constant and loss factor increase with

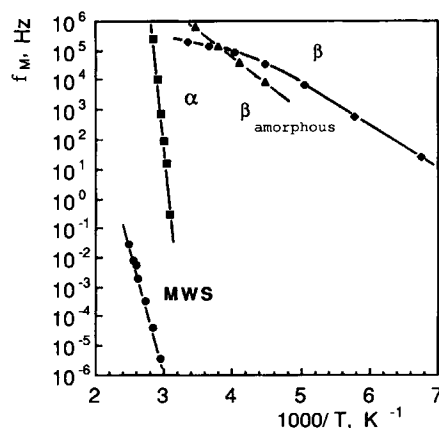


**Figure 7** Transition map of semicrystalline and amorphous PBT.

water absorption, particularly in the high frequency range (according to results elsewhere reported.<sup>16</sup> In Table II, loss factor values (at 25°C in air) at different frequencies and absorbed water contents are reported.

The whole dielectric behavior of semicrystalline PBT is summarized in Figures 8 and 9 by the contour map of loss factor, where the processes previously observed, that is, interfacial polarization (Fig. 8) and  $\alpha$  and  $\beta$  relaxations (Fig. 9), can be easily identified. A three-dimensional map of these relaxations is also reported in Figure 10.

Several features of the dc properties of PBT provide evidence for ionic conduction, as previously pointed out:<sup>1,2</sup>

- (i) The presence of transient phenomena in the dc electrical conductivity curves versus reciprocal absolute temperature (Fig. 1) and their decrease as temperature increases;
- (ii) the non-ohmic behavior of the current-voltage characteristics at temperatures higher than 105°C, even for relatively low electrical fields<sup>2,18</sup>;
- (iii) the systematic decrease of charging currents under low electrical fields after application of higher voltages at 130°C, likely due to sweeping away of charge carriers<sup>2,19</sup>;
- (iv) the conductivity and dielectric losses increase caused by water absorption, although the polymer is intrinsically hydrophobic;
- (v) the onset of a high steady-state current detected in highly amorphous PBT above the glass transition temperature, where ionic transport is enhanced<sup>3</sup>;
- (vi) the observed decrease of dc electrical conductivity with crystallinity.<sup>3</sup>

This last feature can be explained with the higher mobility of ions through amorphous regions in comparison with that in crystalline regions.<sup>20</sup> Indeed, the polymer contains a high concentration of carboxyl end-groups, which can ionize after dissociation of the existing hydrogen bond according to a mechanism proposed for PET,<sup>21</sup> thus providing protons

for conduction. Therefore, mainly above the glass transition temperature, these ionic carriers can migrate in the amorphous regions and accumulate at the interfaces with crystalline regions, giving rise to an interfacial polarization of the Maxwell-Wagner-Sillars type like that previously proposed for PET.<sup>22</sup> Thus, the high temperature peak observed in the electrical conductivity curves of Figure 1 and discharging currents curves of Figure 2, as well as the relaxation process detected in the ultra-low frequency range (Figure 3) and its decrease in the amorphous polymer can be explained.<sup>3</sup> The existence of the Maxwell-Wagner-Sillars polarization is also supported by the ac behavior at high temperature and low frequency: the observed rise of dielectric constant and loss factor with temperature (Figs. 5 and 6) can be related to the enhancement of ion migration in a two-phase crystalline/amorphous system, as found in PET.<sup>23</sup>

Therefore, an essentially ionic (protonic) mechanism of charge transport in PBT can be postulated, mainly at high temperature. However, an electronic contribution, through hopping of charge carriers between localized states, cannot be excluded at low temperature and high electrical fields.<sup>2,24</sup>

As to results of ac measurements, the high-temperature absorption  $\alpha$  (Figure 6) is attributed to large-scale conformational rearrangements of the main chains in the amorphous regions of the polymer (glass transition), while the  $\beta$  relaxation is ascribed to local conformational motions in the chains. Moreover,  $\alpha$  peak in the semicrystalline polymer is smaller in magnitude than that observed in the amorphous PBT.<sup>3</sup> On the contrary, as the amorphous content increases,  $\beta$  relaxation keeps its characteristic broad contour (although it increases in magnitude) and its activation energy does not significantly change. Thus, the  $\beta$  relaxation process must be considered practically independent of morphology, as it generally happens in polymers for local relaxations.<sup>23,25</sup> The presence of these two relaxations is also revealed by the conductivity and discharging currents curves of Figures 1 and 2, where the peaks observed at about -25°C and 40°C can be related to the  $\beta$  and  $\alpha$  processes, respectively.

**Table II Dielectric Loss Factor as a Function of Frequency and Absorbed Water Content**

Wt %	10 <sup>-4</sup> Hz	10 <sup>-3</sup> Hz	10 <sup>-2</sup> Hz	10 <sup>2</sup> Hz	10 <sup>3</sup> Hz	10 <sup>4</sup> Hz	10 <sup>5</sup> Hz
0	0.021	0.013	0.007	0.003	0.004	0.010	0.024
0.13	0.022	0.013	0.007	0.003	0.005	0.012	0.028
0.46	0.055	0.047	0.030	0.006	0.008	0.016	0.040

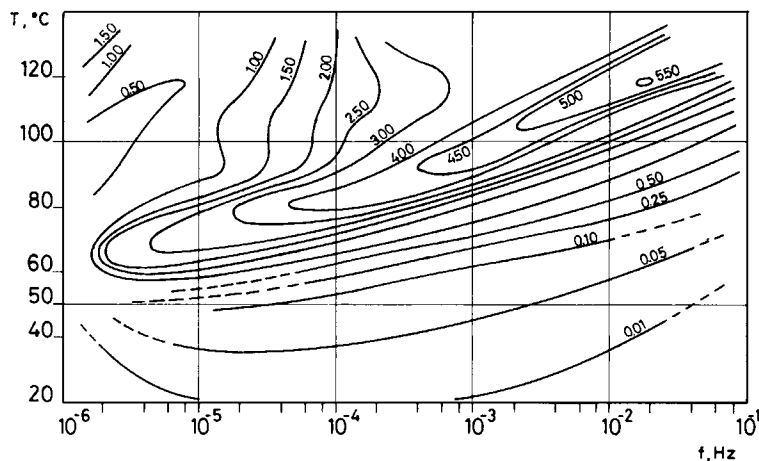


**Figure 8** Loss factor contour map of semicrystalline PBT (ultra-low frequency region).

The contour map of loss factor (Figs. 8–10) summarizes the dielectric behavior of semicrystalline PBT and results in a useful tool for the ac engineering applications of the polymer: PBT insulation can be used with high efficiency essentially in the low loss factor “valley,” i.e. between  $-50$  and  $60^{\circ}\text{C}$ , for power applications, and in a much narrower temperature range for higher frequency applications.

Furthermore, PBT is a highly insulating material, as shown by dc conductivity, and it could also be used at high electrical fields. Dc electrical behavior shows that the polymer can satisfactorily operate continuously at temperature at least up to  $130^{\circ}\text{C}$ , considerably higher than that of other common insulating polymers.

Finally, electrical performances of PBT are

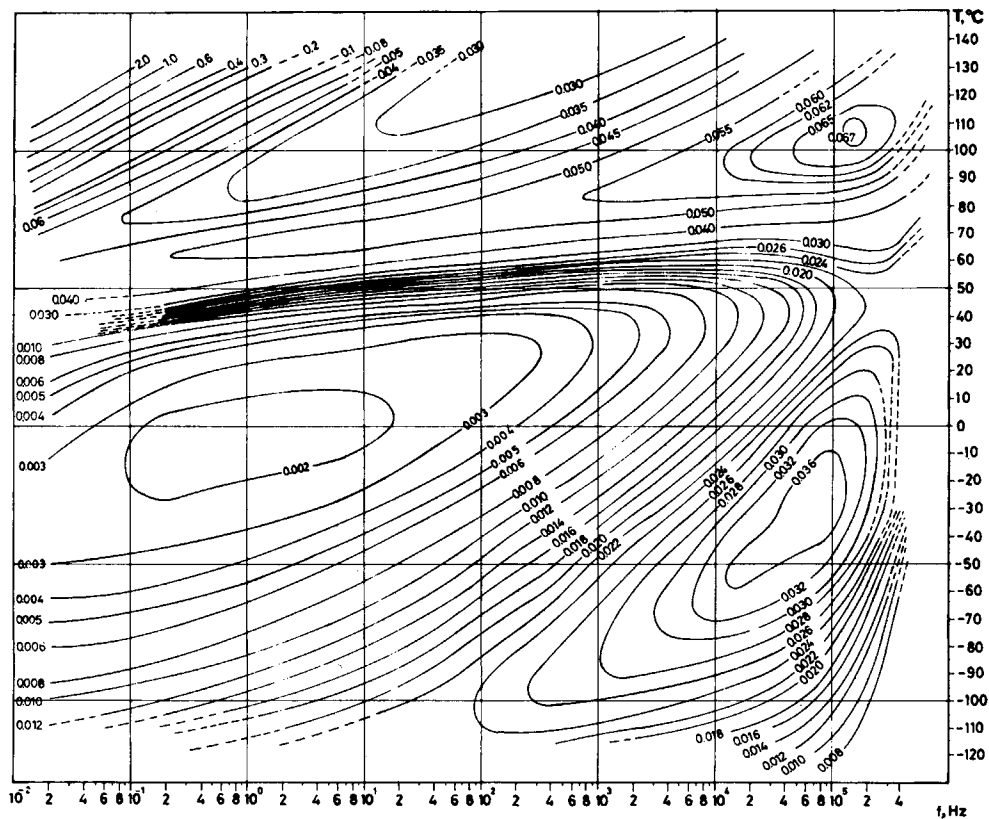


**Figure 9** Loss factor contour map of semicrystalline PBT.

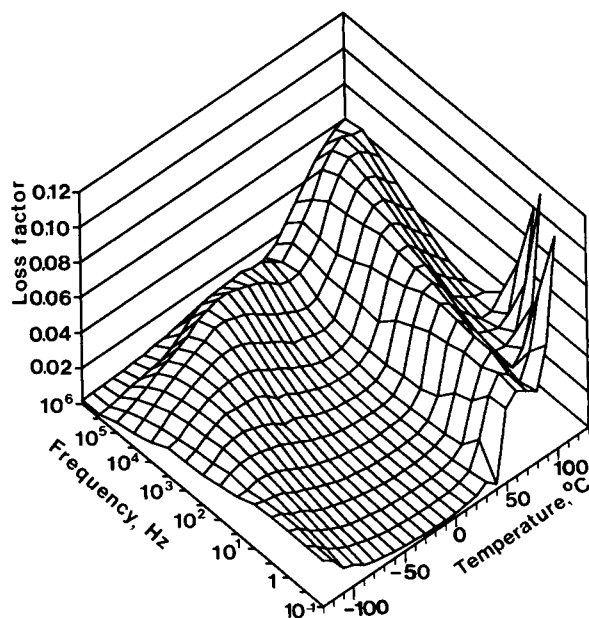


**Figure 10** Loss factor three-dimensional map of semi-crystalline PBT.

somewhat affected by moisture, but to a lesser extent than other polymers: such condition should be, however, carefully taken into account for practical electrical applications.

## CONCLUSIONS

1. An essentially ionic mechanism of conduction can be postulated for PBT. Major charge carriers have been identified in protons supplied by the ionization of carboxyl end-groups after dissociation of the existing hydrogen bonds.
2. Three relaxation processes take place in the polymer, and these must be taken into account for an electrical use of PBT: an  $\alpha$  glass transition, a  $\beta$  subglass relaxation due to local chain motions, and an interfacial polarization of the Maxwell–Wagner–Sillars type.
3. Even low water absorption somewhat enhances ac dielectric losses and dc conductivity, although the polymer is intrinsically hydrophobic: this must be taken into account for electrical applications in moist environments.
4. The contour map of loss factor summarizing the whole dielectric behavior of semicrystalline PBT is an essential tool for the electrical applications of the polymer: practical electrical uses are briefly discussed.

## REFERENCES

1. F. Sandrolini and P. Manaresi, *Proc. 3rd Conv. Ital. Sci. Macromol.*, **19** (1977).
2. F. Sandrolini and P. Manaresi, *Proc. 26th Int. Symp. Macromol.*, IUPAC, Mainz (FRG) Sept. 17, 1979. I. Ludenwald and R. Weis, Eds., Mainz, 1979, Vol. 3, p. 1463.
3. F. Sandrolini and A. Motori, *Proc. 10th Europhysics Conf. Macromol. Phys.*, Noordwijkerhout (The Netherlands) April 21–25, 1980. W. J. Merz, Ed., Eur. Phys. Soc. Publ., Zurich, 1980, Vol. 4A, p. 154.
4. F. Sandrolini, A. Motori, and S. de Petris, *Proc. 27th IUPAC Int. Symp. Macromol.*, Strasbourg (France), July 6–9, 1981, Vol. 2, p. 837.
5. S. de Petris, A. Motori, and F. Sandrolini, in *Interrelations Between Processing, Structure and Properties of Polymeric Materials*. J. C. Seferis and P. S. Theocaris, Eds., Elsevier, Amsterdam, 1984, p. 511.
6. O. S. Gal and P. Premovic, *Die Angew. Makromol. Chem.*, **84**, 1, (1980).
7. F. Sandrolini, *J. Phys. E. Sci. Instr.*, **13**, 152 (1980).
8. B. V. Hamon, *Proc. IEE*, **99**(Pt. IV), 151 (1952).
9. M. E. Baird, *Prog. Polym. Sci.*, **1**, 161 (1967).
10. H. Block, R. Groves, P. W. Lord, and S. M. Walker, *J. Chem. Soc., Faraday Trans. 2*, **68**, 1890 (1972).
11. H. J. Wintle, *Solid-State Electronics*, **18**, 1039 (1975).
12. F. Sandrolini, *Proc. Seminar Il comportamento elettrico dei materiali polimerici (Electrical behaviour of polymeric materials)*. Bologna, March 1–2, 1984, Pi-tagora-Tecnoprint, Ed., Bologna, 1984, p. 247.
13. M. E. Baird, *Rev. Mod. Phys.*, **40**, 219 (1968).
14. H. J. Wintle, *J. Non-Cryst. Solids* **15**, 471 (1974).
15. F. Sandrolini and P. Cremonini, *Mat. Plast. Elastom.*, **7–8**, 3 (1979).
16. E. Ito and Y. Kobayashi, *J. Appl. Polym. Sci.*, **25**, 2145 (1980).
17. W. P. Leung and C. L. Choy, *J. Appl. Polym. Sci.*, **27**, 2693 (1982).
18. M. E. Baird, *Electrical properties of polymeric materials*. The Plastic Inst., London, 1973.
19. E. Sacher, *J. Phys. D*, **5**, L 17 (1972).
20. A. R. Blithe, *Electrical properties of polymers*. Cambridge Univ. Press, Cambridge, 1979.
21. E. Sacher, *J. Macromol. Sci., Phys. B*, **4**, 441 (1970).
22. D. K. Das Gupta and K. Joyner, *J. Phys. D*, **9**, 829 (1976).
23. J. C. Coburn and R. H. Boyd, *Macromolecules*, **19**, 2238 (1986).
24. T. J. Lewis, *Sci. Pap. Inst. Org. Phys. Chem.*, Wroclaw Tech. Univ., Nr. 7 Ser., Conf. n° 1, p. 146 (1972).
25. R. H. Boyd, *Polymer*, **26**, 323 (1985).

Received December 28, 1990

Accepted March 29, 1991